Harper–Dorn Creep and Specimen Size

E. NES, W. BLUM, and P. EISENLOHR

Under conditions typical of Harper–Dorn (H–D) creep the statistical slip-length may become comparable to, or even exceed, the specimen diameter (a size effect). It is demonstrated that a consequence of such a size effect is that the rates of dislocation storage and dynamic recovery are reduced and the static recovery rate will exceed the dynamic one. Under such conditions, the analysis shows that the creep rate will scale linearly with the applied stress, a characteristic of H–D creep.

I. INTRODUCTION

HARPER–DORN (H–D) creep was first reported in 1957 by Harper and Dorn,[1] who tested tensile specimens of both single and polycrystalline pure aluminum (99.99) at very low stresses and at temperatures near the melting point. Since then, the phenomenon has been subjected to numerous experimental and theoretical investigations. From the creep literature (for reviews, see References 2 through 5) the primary characteristics of H–D creep can be summarized as follows. (a) H–D creep is a steady-state phenomenon. (b) The stress exponent is, as in Nabarro–Herring creep, equal to 1, but the kinetics can be more than two orders of magnitude faster than this variant of diffusion creep. (c) The activation energy of H–D creep is close to that of self-diffusion. (d) The phenomenon is commonly interpreted in terms of a dislocation mechanism. (e) The dislocation density is very low (of the order $5 \cdot 10^7$ m^{-2}) and independent of stress. Most recently, however, the phenomenon has been subjected to a somewhat more critical re-examination. New experiments cast doubt about its existence, as experiments by Blum *et al.*[6,7] on high purity aluminum showed no evidence of this low stress deviation from power-law creep (Figure 1). Blum *et al.* performed compression experiments on specimens of much larger cross section than commonly used; accordingly, they opened for speculation the interpretation of H–D creep as a size effect.[7] Ginter *et al.*[8] and Mohamed[5] suggest that a pure dislocation mechanism may be insufficient in the interpretation of this creep phenomenon, and these authors also contribute to speculations about its transient nature. The purpose of this article is to explore the new idea that the occurrence of H–D creep is a *size effect*. The model to be developed is of a general character, but the application considered will be limited to H–D creep observations in aluminum. Since the model to be presented relies on a dislocation network description, the model and observations of Ardell and co-workers[9,10,11] are of some relevance in this context; accordingly, some aspects of their network model and observations will be briefly reviewed first.

E. NES, Professor, is with the Department of Materials Technology and Electrochemistry, Norwegian University of Science and Technology, 7034 Trondheim, Norway. W. BLUM, Professor, and P. EISENLOHR, Graduate Student, are with the Institut fur Werkstoffwissenschaften LS 1, University of Erlangen, 91058 Erlangen, Germany.

This article is based on a presentation made in the workshop entitled "Mechanisms of Elevated Temperature Plasticity and Fracture," which was held June 27–29, 2001, in San Diego, CA, concurrent with the 2001 Joint Applied Mechanics and Materials Summer Conference. The workshop was sponsored by Basic Energy Sciences of the United States Department of Energy.

II. NETWORK MODEL

Ardell and co-workers[9,10,11] have developed a network model, which they claim explains both the transient primary-creep stage and the subsequent H–D creep. The transient starts, according to their observations, with a dislocation burst on loading, resulting in an initial high strain rate and dislocation density, followed by a rapid decay in both quantities.[10] This dislocation decay is interpreted in terms of network growth, a phenomenon, which according to experimental observations, rapidly stagnates and renders a steady-state Frank network accommodating H–D creep. This stagnation is interpreted in terms of a "frustration phenomenon" induced by enforcing Frank's rule at the nodes.[10] The physics of this growth reaction is less clear. In terms of common interpretations of the growth of a two-dimensional network, Figure 2(a), loops that are made up of many link-length segments will expand due to the shrinkage of those with fewer, in analogy with grain growth. The driving force for the reaction results from elastic interactions due to the dislocation stress fields in combination with nodes trying to maintain local line-tension equilibrium (Figure 2(b)). Collapse of such loops will, of course, never violate Frank's rule, and without any other restriction imposed, this network can never be "frustrated." Network growth, however, may stagnate due to other reasons. In the present situation, the effect of the 10 to 100 ppm of impurities in solid solution will have such an effect. The problem, however, of understanding the network model for H–D creep does not pertain to the establishment of a quasi stationary network due to dislocation interactions and line-tension forces but to how such a network can accommodate the observed metal plasticity without the operation of dislocation sources to maintain a steady-state dislocation density. No simple physical picture has been presented by Ardell and co-workers, as a background for their lengthy derivations developed to prove H–D creep.[9,11] Further, no convincing argument has been provided for how such a network satisfies the boundary conditions imposed by the Orowan relationship:

$$\dot{\gamma} = b\rho_m v \qquad [1]$$

where $\dot{\gamma}$ is the shear strain rate, ρ_m is the density of mobile dislocations, b is the Burgers vector length, and v is the average speed of the mobile dislocations. Since the Ardell

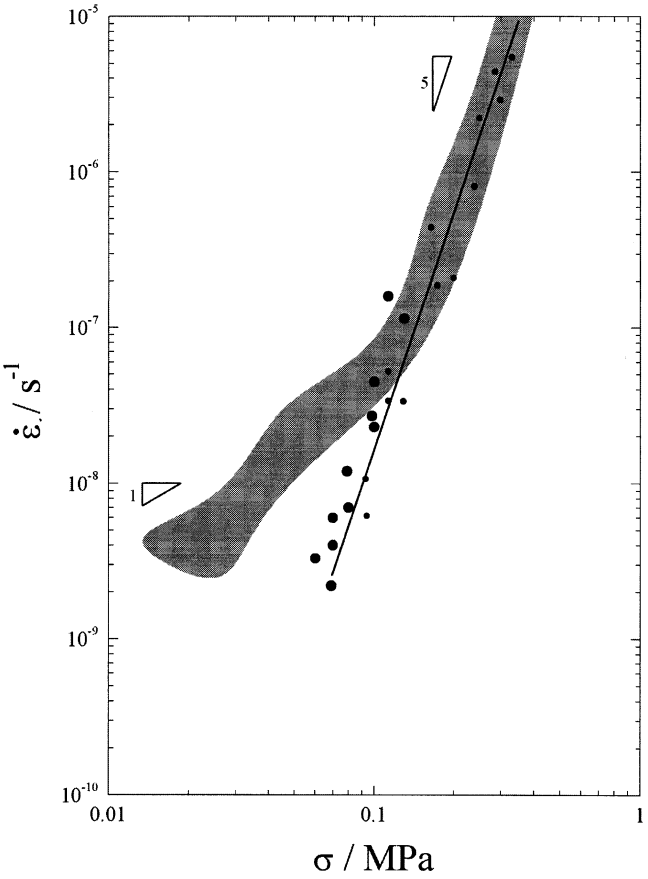

Fig. 1—Creep rate ($\dot{\varepsilon}$) of pure Al as a function of normal stress (σ) at 923 K, as reported in Ref. 7. Small circles: steady-state compressive creep rates measured with rod/tube extensometers,[6] large circles: compressive creep rates measured with contactless laser extensometer at some distance from steady state in primary transient creep,[7] and shaded area: tensile creep rates from literature, as collected in Ref. 6.

model[9,10,11] excludes mobile dislocations due to the operation of dislocation sources, the network itself must, in addition to being a stable Frank configuration, also act in a dynamic way providing the mobile dislocations required in order to satisfy Eq. [1]. Or, in other words, the total number of segments in the Frank network must migrate in a concerted manner in such a way that the Orowan relation is obeyed. Selecting typical values for the strain rate and the dislocation density during H–D creep, this average speed becomes of the order 10 μm/s. How such a migration pattern can be reconciled with a stable network is difficult to understand. Its consequence, in the absence of active sources, seems to be that most segments will have left the specimen in about 1000 seconds. However, as will be shown in the following section, the observations of Ardell and co-workers can be rationalized in terms of a *size effect*, the result of which is the change in power-law creep exponent from 4 to 1, the latter typical of H–D creep.

III. HARPER–DORN CREEP, A SIZE EFFECT

A. *Dislocation Structure Evolution*

The H–D creep experiments, conducted on nearly dislocation-free specimens of high purity aluminum at temperatures close to the melting point, result upon loading in a strain

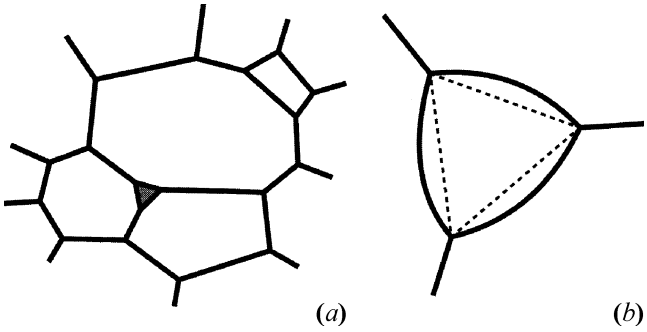

Fig. 2—(*a*) Two-dimensional dislocation network. The individual loops contain different numbers of links. (*b*) Instable loop consisting of three segments. Solid lines represent nodal force equilibrium. Concurrent minimization of dislocation curvature (dashed lines) disturbs the nodal force balance, which leads to shrinkage and eventually collapse of the loop.

burst introducing a relatively high density of initially mobile dislocations, as demonstrated by the investigation by Ardell and co-workers. The way these dislocations contribute to strengthening is given in terms of resolved shear stresses by

$$\tau = \tau_t + \hat{\tau} \qquad [2]$$

where τ is the applied stress, τ_t is the thermal stress component, and $\hat{\tau}$ is the athermal component. Since strengthening under these conditions seems to be affected by subgrains to a marginal extent only,[9] the athermal strength contributions can be calculated on the basis of a one-parameter description in a standard way; *i.e.*, this component becomes

$$\hat{\tau} = \alpha G b \sqrt{\rho} \qquad [3]$$

where α is a constant ($\approx$0.3), G is the shear modulus, and ρ is the density of *stored* dislocations.

In order to follow the transition towards a steady-state condition, the dislocation evolution equation needs to be solved. This important problem has recently been considered by Nes and co-workers,[13–16] from which treatments of only the aspects relevant in the present context will be briefly reviewed. Previous treatments, however, neglected the effect of *static recovery* on the network evolution during plastic deformation, the reason for this being that the static contribution, for good reasons, is generally assumed to be significantly lower than the dynamic one. This is, as will be shown subsequently, not necessarily the case under such extreme conditions typical of H–D creep.

Under the dynamic conditions of metal plasticity, the network evolution ($\dot{\rho}$) is commonly analyzed in terms of the combined result of athermal storage of dislocations ($\dot{\rho}^+$) and dynamic recovery ($\dot{\rho}^-$); *i.e.*,

$$\dot{\rho} = \dot{\rho}^+ + \dot{\rho}^- \qquad [4]$$

Dislocations are stored, due to interactions between already stored segments in the Frank network and mobile dislocations, at the rate

$$\dot{\rho}^+ = \frac{2}{bL}\,\dot{\gamma}, \text{ where } L = \frac{C}{\sqrt{\rho}} \qquad [5]$$

and $C > 1$ is a numerical constant. The quantity L represents the average distance a mobile dislocation migrates from the source to the site where it is stored in the network; Reference 13 gives detailed statistical analysis.

B. *Static vs Dynamic Recovery*

Dynamic recovery is commonly interpreted as the result of local annihilation reactions between mobile dislocations and stored dislocation segments in the Frank network.[13–18] Under dynamic conditions such annihilation reactions are assumed to destabilize the evolving network much more effectively than network growth due to the stored line energy, *i.e.*, static recovery. In principle, however, the latter contribution to recovery should be included, as was done in an earlier treatment by Estrin.[19] Further, as will be demonstrated in the following, under extreme conditions, such as close to the melting point (H–D creep), static recovery may even contribute more effectively to network growth than dynamic recovery. Accordingly, the total recovery reaction during metal plasticity becomes

$$\dot{\rho}^{-} = \dot{\rho}^{-}_{\text{dynamic}} + \dot{\rho}^{-}_{\text{static}} \qquad [6]$$

The dynamic recovery model for a Frank dislocation network developed by Nes and Marthinsen[13–16] is based on the assumption that network growth is controlled by the collapse of dislocation dipoles of separation l_g where the dipole configurations are the result of interactions between the stored network dislocations and mobile ones. It follows that l_g is expected to be much smaller than the average separation of stored dislocations, *i.e.*, $l_g = 1/\xi\sqrt{\rho}$ where ξ is a scaling parameter $\gg 1$. The collapse rate of dipoles will result in a dynamic recovery rate given by

$$\dot{\rho}^{-}_{\text{dynamic}} = -v_g\rho \qquad [7]$$

where v_g is the dislocation collapse frequency. In pure metals, where climb is expected to be rate controlling, the collapse reaction is expected to be driven by the sharp curvatures resulting from dipole pinch-off reactions (References 14 and 16). The pinched-off segments will then rapidly climb sidewise due to large curvature forces. The collapse frequency then becomes $v_g = 2v_c\sqrt{\rho}$, where v_c is the climb speed given by

$$\begin{aligned} v_c &= v_D b^2 B_\rho c_j \exp\left(-\frac{U_{SD}}{kT}\right) 2 \sinh\frac{Fb^2}{kT} \\ &\approx 2\, v_D b^2 B_\rho c_j \left(\frac{Fb^2}{kT}\right) \exp\left(-\frac{U_{SD}}{kT}\right) \end{aligned} \qquad [8]$$

where v_D = Debye frequency, U_{SD} = activation energy for selfdiffusion and T = temperature.

The curved segments generate a driving force, $F = 2\Gamma/l_g = 2\Gamma\xi\sqrt{\rho}$, where Γ is the dislocation line tension ($\Gamma = (Gb^2/4\pi(1-\nu)\ln(1/b\sqrt{\rho}) \approx 1.7Gb^2$, for $\rho \approx 10^7$ m^{-2}), B_ρ is a constant of order unity, and c_j represents the concentration of trailing jogs controlling the climb rate of the curved segments, *i.e.*, $c_j = 1/l_j$, where l_j is the separation of trailing jogs, a quantity that is expected to scale with the dipole separation. Typical ξ values are of the order 30 (*as discussed subsequently*), which implies that $F \approx 100\,\sigma\, b$ (σ: applied normal stress). Under such high driving forces, vacancy equilibrium is not expected to be established at the jogs, and it follows from Reference 12 that the jog climb-rate under such conditions takes the form expressed by Eq. [8]. For more details, see References 13 through 16.

It follows from the classic treatments by Friedel[20] and Hirth and Lothe[12] that the growth of the Frank network due to line-tension forces will cause an additional recovery rate written in the form

$$\dot{\rho}^{-}_{\text{static}} = -B_{FN}\rho^2\left(\frac{Gb^3}{kT}\right)D_{SD} \qquad [9]$$

where D_{SD} is the self-diffusion parameter, and $B_{FN} = B^0_{FN}\, 2\pi/\ln(1/b\sqrt{\rho})$ where B^0_{FN} is a parameter of order unity. Under steady-state conditions ($\dot{\rho} = 0$), combination of Eqs. [2] and [4] through [8] (assuming $\tau_t \ll \tau$) results in a constitutive law for power-law creep with the stress exponent equal to 4[13,14,16] when the effect of static recovery can be neglected; for further comments on the static recovery effect, see the subsequent *discussion*. However, if the temperature is increased, approaching that of the melting point (H–D region), the dislocation density will decrease to very low levels. The consequence becomes that the slip-length, L, will increase, and a situation will eventually emerge where the slip-length becomes comparable to or even larger than the specimen diameter. When such a situation arises, the specimen size will affect both the storage rate of dislocations and their dynamic recovery rate, *i.e.*, a *size effect* has been established.

C. *A Size Effect*

The effect of reducing the specimen cross section on the substructure evolution can be analyzed in an approximate way by redefining Eq. [5] as follows:

$$\dot{\rho}^{+} = S\,\frac{2}{bL}\,\dot{\gamma}, \text{ with } S = \frac{R^2}{((R+L)^2 - R^2)\lambda + R^2} \qquad [10]$$

where R is the specimen radius, and λ is a parameter expected to be of the order 1 (reflecting surface conditions). The idea behind this S parameter is that when the slip-length becomes comparable to, or larger than, the specimen radius, then, Eq. [6] no longer is valid since this relationship then will include the effect of sources located in an area ($(R+L)^2 - R^2$) outside the specimen, *i.e.*, phantom sources. By multiplying by S at the right side in Eq. [5], the effect of these phantom sources is excluded.* This S parameter, however, should capture the salient physical consequence of a size effect with the boundary conditions satisfied; *i.e.*, when $L \ll R$, $S \to 1$, and when $L \gg R$, $S \to 0$; the latter case corresponds to no storage at all, as expected.

*The introduction of this S parameter is consistent with the statistical treatment of the dislocation storage problem presented in Reference 13, in the sense that S (not $S^{1/2}$) appears in Eq. [10]. An extension of this statistical treatment to include the size effect is a difficult problem, indeed.

The dynamic recovery rate will be affected in an analogous way. As the storage rate decreases, the density of dipole configurations will necessarily decrease, with the reduction rate per unit volume expected to scale with $S^{3/2}$. And, it follows that Eq. [7] takes the form

$$\dot{\rho}^{-}_{\text{dynamic}} = -S^{3/2}v_g\rho \qquad [11]$$

This relationship satisfies the boundary conditions, *i.e.*, if $L \ll R$, Eq. [11] becomes equal to Eq. [7], and if $L \gg R$, the dynamic recovery rate approaches zero. The static recovery rate will, of course, not be affected by any size effect. By solving the microstructural evolution law under steady-state conditions, $\dot{\rho} = 0$, *i.e.*, by combining Eqs. [4],

[6], and [8] through [11], the effect of specimen size on the creep rate becomes

$$\dot{\gamma} = \frac{bC}{2}\frac{Gb^3}{kT}\left(\frac{B_{FN}}{S}\rho^{3/2} D_{SD} + \sqrt{S}\ 13.6\ b^3\xi^2 B_\rho \rho^2 \nu_D \exp\left(-\frac{U_{SD}}{kT}\right)\right) \quad [12]$$

As long as the thermal component of the flow stress is negligible so that $\hat{\tau} \approx \tau$, one finds from Eqs. [3] and [12] that

$$\dot{\gamma} = \frac{C}{2\alpha^3 b^2}\left(\frac{Gb^3}{kT}\right)\left[\frac{B_{FN}}{S}\left(\frac{\tau}{G}\right)^3 D_{SD} + \sqrt{S}\,\frac{13.6b^2}{\alpha}\,\xi^2 B_\rho \left(\frac{\tau}{G}\right)^4 \nu_D \exp\left(-\frac{U_{SD}}{kT}\right)\right] \quad [13]$$

Under conditions where $L \gg R$ (and $\lambda \approx 1$), this equation reduces to

$$\dot{\gamma} = \frac{C^3}{2\alpha}\frac{Gb^3}{kT} D_{SD}\frac{B_{FN}}{R^2}\frac{\tau}{G} \quad [14]$$

which is a constitutive relationship rationalizing H–D creep.

The model prediction according to Eq. [13] is shown in Figure 3 for a specimen diameter of 12 mm. The parameter values used are $D_{SD} = 1.76 \cdot 10^{-5}$ exp $(-U_{SD}/RT)$ m^2/s,[21] $U_{SD} = 126153$ J/mol,[21] $G = 2.99 \cdot 10^4$ exp $(-5.4 \cdot 10^{-4} \cdot T/k$ *MPa*, $\nu_D = 10^{13}$ s^{-1}, $\alpha = 0.3$, $C = 100$, $B^0_{FN} = 0.01$, $B_\rho = 3$, $\lambda = 1$, and $\xi = 30$, (λ, B^0_{FN}, and B_ρ are the only fitting parameters involved, and the values used for those are reasonable (References 14 and 16)). The choice was done such that the model curve fits the low-stress tensile data (shaded area) from specimens with diameters of about $\frac{1}{2}$ inch. At relatively high stresses, the dynamic recovery contribution is dominant; at low stresses, the static one dominates. The broken line in Figure 3 shows the creep-rate contribution caused by static recovery *in the absence* of a size effect, and the conclusion becomes that creep controlled by static recovery will in general only be detectable under conditions where the specimen diameter becomes comparable to or smaller than the slip length (size effect).

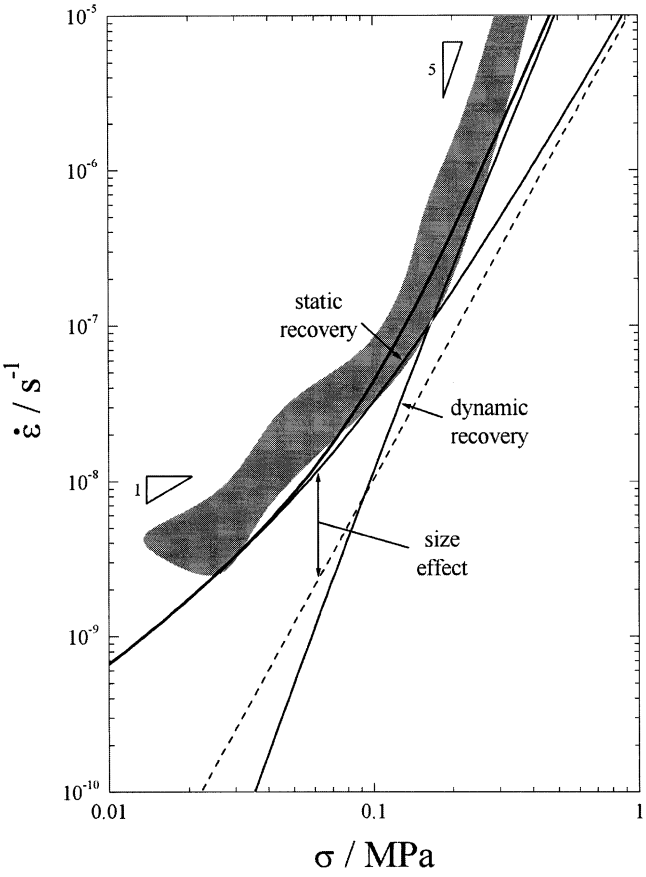

Fig. 3—Steady-state creep rates as modeled by Eq. [13] for a specimen with 12 mm diameter in dependence of normal stress at 923 K ($\gamma/\dot{\varepsilon} = \sigma/\tau = 3$). The contributions from dynamic and static recovery dominate at high and low stresses, respectively. The broken line shows the steady-state creep rate due to static recovery in the absence of a size effect. Shaded area: as in Fig. 1.

D. *The Dislocation Density Aspect*

As pointed out in the introduction, it follows from the creep literature that a characteristic aspect of H–D creep is a strain-rate invariant dislocation density. However, the size effect model presented in the previous section does not predict such a creep-behavior in the H–D region. To the contrary, by solving the substructure evolution law (Eq. [4]) under steady-state conditions and with $L \gg R$, the prediction becomes that $\sqrt{\rho} \propto \dot{\gamma}$. As pointed out in Reference 13, a strain-rate, (or stress) invariant, constant steady-state dislocation density cannot be reconciled with an appropriate solution of Eq. [4], *i.e.*, such a condition is in conflict with the laws of physics governing steady-state conditions. Two possibilities then remain; either the H–D creep is not a true steady-state phenomenon (a transient), or the dislocation density measurements are not accurate enough. The latter possibility needs to be considered for the following reason. It is the personal experience of one of the present authors[13,22] that the handling of high purity aluminum with dislocation densities of 10^7 m^{-2} or less (flow stresses of less than 1 g/mm^2) probably is not possible without introducing additional dislocations during demounting, transportation, and polishing of the specimens. A dislocation density of $5 \cdot 10^7$ m^{-2}, reported to be the typical level of H–D creep, may simply reflect the lowest possible dislocation density to be revealed by etch-pit techniques.

E. *Metal Purity and Experimental Conditions*

It needs to be pointed out that commercial high purity grades of aluminum used in H–D creep experiments are not high purity metals in the true meaning of the word. This becomes particularly relevant under such extreme conditions, as those prevailing under H–D creep. This probably explains the considerable spread in experimental data when comparing results from different groups, as shown in Figures 1 and 3. For an interesting review of impurity effects, see Reference 5. In the investigation of a possible size effect, it becomes important that only one grade of high purity aluminum is tested.

IV. DISCUSSION

It has been shown that the high creep rates during H–D creep may result from a size effect. The effect rests on

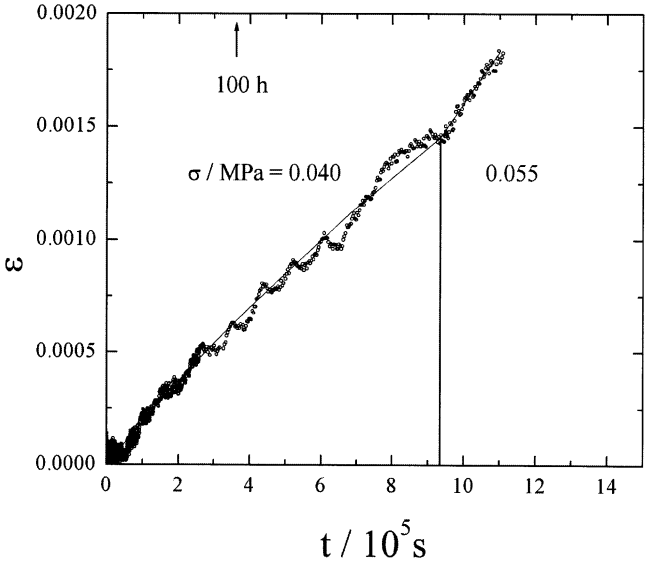

Fig. 4—Strain-time curve from the compression test with the specimen of 11 mm side length and aspect ratio of 2 at 923 K and 0.040 MPa with an increase in stress to 0.055 MPa.

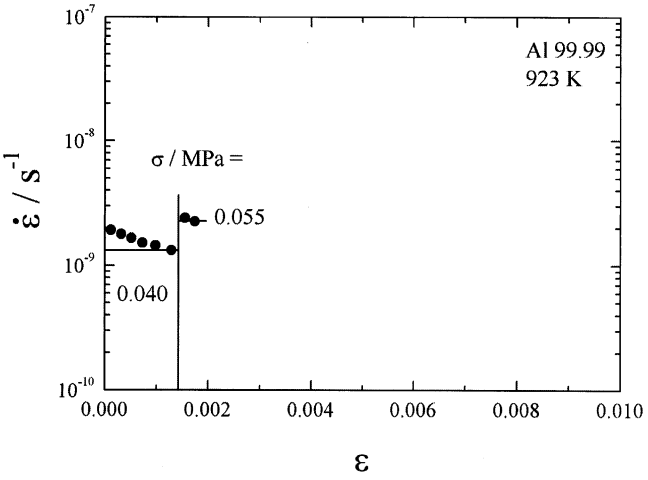

Fig. 5—Creep rate-strain curve from the compression test of Fig. 4. Creep rate is calculated from the slope of the smoothed line in Fig. 4.

the assumption that the surface of Al specimens does not represent a barrier dislocations. This assumption appears reasonable in view of the extremly small volume fraction of the oxide shell. It has also been confirmed experimentally by Nøst and Nes,[22] their *in-situ* X-ray topography investigation of aluminum crystals under load clearly revealed that the surfaces acted as perfect sinks for the mobile dislocations. Note that the specimen size effect differs from the grain size effect. Due to compatibility requirements, dislocations are not free to leave the grains at the boundaries. In this case, there is a reduction in slip distance, L, with reduction in grain size, leading to a decrease in steady-state creep rate in opposition to the specimen size effect occurring under H–D creep conditions.[15,16]

The fit of the model curve to the experimental data in Figure 3 becomes imperfect as the stress increases. The reason is simply that the dynamic recovery term is connected with a stress exponent of 4, while $n = 5$ is observed experimentally. There is a need to improve the description of creep in that range. The important point to be emphasized here is that a size effect is predicted in the low stress range of H–D creep.

The size effect has to be checked by independent measurements. It should be noted that in cubical compression specimens the dislocations are not free to leave the surfaces because their glide planes usually intersect the compression faces. Therefore, tensile tests on long specimens with different diameters appear to be most suitable to test the size effect. Recently, McKnee *et al.*[23] have reported that they could not generally confirm H–D creep except for a few cases. Unfortunately, the specimen sizes were not given in their work so that a size effect is not excluded.

An effort was made within the present work to demonstrate the predicted size effect experimentally. For this purpose, a tall compression specimen with a cross section of 11 mm × 11 mm and an aspect ratio of 2.3 was deformed at 0.040 MPa and 923 K. Length measurement was done with a laser extensometer. The accuracy of the extensometer was inadvertently demonstrated by a slow decrease in test

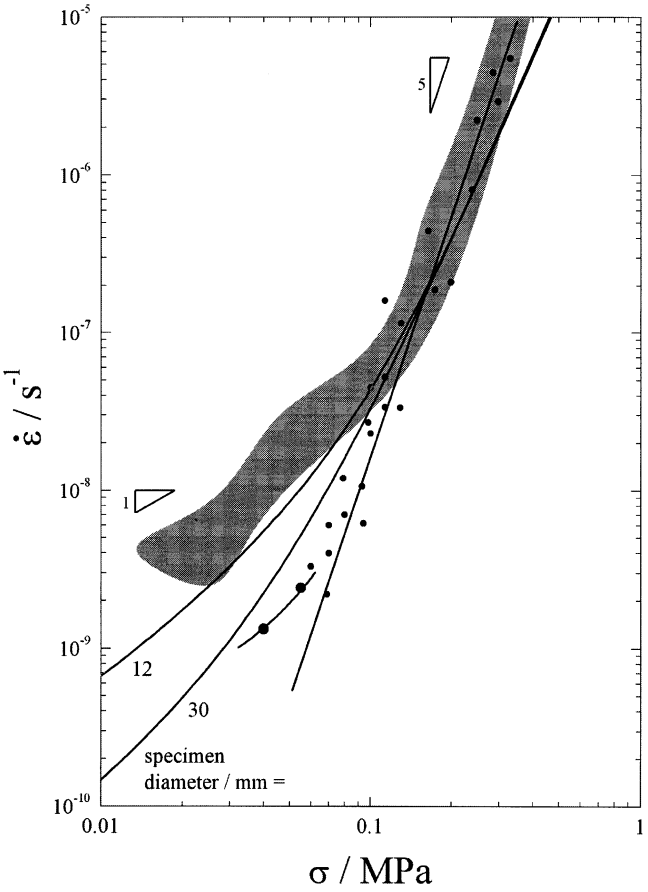

Fig. 6—Model curves for specimens of 12 and 30 mm diameter and compression creep data for specimens with 11 mm (large circles) and 29-mm (small circles) side length.

temperature by 4 K, which led to the thermal contraction expected from the expansion coefficient of pure Al. Figure 4 shows the strain-time response. After nearly 300 hours, the stress was increased to 0.055 MPa. Figure 5 shows the creep rate, $\dot{\varepsilon}$, as function of creep strain ε. There is no indication of a primary range of creep with decrease of $\dot{\varepsilon}$ within the small ε interval investigated. The creep rates

corresponding to the horizontal lines of Figure 5 are shown in Figure 6 as large full circles. They indicate a deviation from the straight line derived from the data points of Figure 1 obtained from big, nearly cubical specimens. It is interesting to note that they also agree very well with the results of McKnee *et al.* measured in tensile tests.[23] The size effect should cause a difference by a factor of 2 to 3 between the steady-state creep rates of specimens with 12 and 30 mm diameter at a stress of 0.04 MPa (*cf.* Figure 6). This is consistent with the distance by which the experimental data for compression specimens with 11 mm side length differ from the line for compression specimens with 29 mm side length at 0.04 MPa. The slope of the line for the 11-mm compression specimens agrees closely to the slope of the model line for 12-mm diameter. It is concluded that the present test supports the size effect not only from the absolute magnitude but also from the low stress dependence of the creep rate.

V. SUMMARY

A simple model has been proposed that predicts an effect of specimen size on the steady-state creep rate at very low stresses, where the slip distance of gliding dislocations becomes comparable to the specimen diameter. The effect results from the laws of dislocation-structure evolution through a reduction of the rates of dislocation storage as well as of dynamic dislocation recovery in the presence of static recovery of the dislocation network, which due to its localized nature is insensitive to specimen size. The result is that the steady-state density of dislocations is reduced, and the steady-state creep rate is increased with reduced specimen cross section. The effect becomes more pronounced with decreasing stress and increasing dislocation-structural dimensions. In this way, the stress exponent is decreased from a value in the order of 4 to 5 to a value near 1. A test with a tall compression specimen having a relatively large aspect ration of 2.03 at low stresses confirms the existence of a size effect not only by the absolute magnitude of the creep rate but also by the low stress exponent. The size effect explains the well known H–D creep behavior.

ACKNOWLEDGMENTS

This work is a result of discussions under a recent Creep Workshop held as part of the MMC-conference in San Diego, June 2001. The authors thank the participants in this workshop, particularly the organizer, Professor M. Kassner. Thanks are also due to Professor K. Marthinsen. Financial support by the Bundesministerium für Bildung und Forschung and Schott Lithotec AG is gratefully acknowledged.

REFERENCES

1. J. Harper and J.E. Dorn: *Acta Metall.*, 1957, vol. 5, p. 654.
2. J. Cadec: *Creep in Metallic Materials*, Elsevier, Amsterdam, 1988.
3. H. Oikawa and T.G. Langdon: in *Creep Behavior of Crystralline Solids*, B. Wishire and R.W. Evans, eds., Pineridge Press, Swansea, 1985, pp. 33-82.
4. F.A. Mohamed and J. Wolfenstine: in *Creep Deformation of Aluminum Alloys*, T.G. Langdon, H.P. Merchant, J.D. Morris, and M.A. Zaidi, eds., TMS, Warrendale, PA, 1991, pp. 223-37.
5. F.A. Mohamed: *Metall. Mater. Trans. A*, 2002, vol. 33A, pp. 261-78.
6. W. Blum and W. Maier: *Phys. Status Solidi (a)*, 1999, vol. 171, pp. 467-74.
7. W. Blum, P. Eisenlohr, and F. Breutinger: *Metall. Mater. Trans. A*, 2002, vol. 33A, pp. 291-303.
8. T.J. Ginter, P.K. Chaudhury, and F.A. Mohamed: *Acta Mater.*, 2001, vol. 49, pp. 263-272.
9. A.J. Ardell and S.S. Lee: *Acta Metall.*, 1986, vol. 34, pp. 2411-23.
10. A.J. Ardell: *Acta Mater.* 1996, vol. 45, pp. 2971-81.
11. M.A. Przystupa and A.R. Ardell: in *Deformation, and Properties of Structural Materials*, E.M. Taleff, C.K. Syn, and D.R. Lesner, eds., TMS, Warrendale, PA, 2000, pp. 157-68.
12. J.P. Hirth and J. Lothe: *Theory of Dislocations*, McGraw-Hill, New York, NY, 1968.
13. E. Nes: *Progr. Mater. Sci.*, 1998, vol. 41, p. 129.
14. E. Nes, T. Pettersen, and K. Marthinsen: *Scripta Mater.*, 2000, vol. 43, p. 55.
15. K. Marthinsen and E. Nes: *Mater. Sci. Technol.*, 2001, vol. 17, p. 376.
16. K. Marthinsen and E. Nes: *Mater. Sci. Eng.*, in press.
17. U.F. Kocks: *J. Eng. Mater. Technol. (ASME-H)*, 1976, vol. 98, p. 76.
18. H. Mecking and U.F. Kocks: *Acta Metall.*, 1981, vol. 29, p. 1865.
19. Y. Estrin: in *Unified Constitutive Laws of Plastic Deformation*, A.S. Krausz and K. Krausz, eds., Academic Press, New York, NY, 1996, pp. 69-106.
20. J. Friedel: *Dislocations and Mechanical Properties of Crystals*, Wiley, New York, NY, 1957.
21. T.E. Volin, K.H. Lie, and R.W. Balluffi: *Acta Metall.*, 1971, vol. 19, p. 264.
22. B. Nøst and E. Nes: *Acta Metall.*, 1969, vol. 17, pp. 13-20.
23. K.R. McKnee, H. Jones, and G.W. Greenwood: *Proc. 9th Int. Conf. on Creep and Fracture of Engineering Materials and Structures*, J.D. Parker, ed., The Institute of Metals, London, 2001, pp. 185-95..